Eur. Phys. J. A **14**, 469–475 (2002)
DOI 10.1140/epja/i2002-10031-y

THE EUROPEAN PHYSICAL JOURNAL A

Microscopic three-body force for asymmetric nuclear matter

W. Zuo[1], A. Lejeune[2], U. Lombardo[3,a], and J.F. Mathiot[4]

[1] Institute of Modern Physics, Chinese Academy of Sciences, 730000 Lanzhou, PRC
[2] Institut de Physique, B5 Sart-Tilman, B-4000 Liège 1, Belgium
[3] Dipartimento di Fisica, 57 Corso Italia, and INFN-LNS, 44 Via Santa Sofia, 95125 Catania, Italy
[4] Laboratoire de Physique Corpusculaire, Université Blaise-Pascal, CNRS-IN2P3, 24 Avenue des Landais, F-63177 Aubiere Cedex, France

Received: 18 February 2002 / Revised version: 25 April 2002
Communicated by P. Schuck

Abstract. Brueckner calculations including a microscopic three-body force have been extended to isospin-asymmetric nuclear matter. The effects of the three-body force on the equation of state and on the single-particle properties of nuclear matter are discussed with a view to possible applications in nuclear physics and astrophysics. It is shown that, even in the presence of the three-body force, the empirical parabolic law of the energy per nucleon *vs.* isospin asymmetry $\beta = (N - Z)/A$ is fulfilled in the whole asymmetry range $0 \leq \beta \leq 1$ up to high densities. The three-body force provides a strong enhancement of the symmetry energy which increases with density in good agreement with the predictions of relativistic approaches. The Lane's assumption that proton and neutron mean fields linearly vary *vs.* the isospin parameter is violated at high density due to the three-body force, while the momentum dependence of the mean fields turns out to be only weakly affected. Consequently, a linear isospin split of the neutron and proton effective masses is found for both cases with and without the three-body force. The isospin effects on multifragmentation events and collective flows in heavy-ion collisions are briefly discussed along with the conditions for direct URCA processes to occur in the neutron star cooling.

PACS. 25.70.-z Low and intermediate energy heavy-ion reactions – 13.75.Cs Nucleon-nucleon interactions (including antinucleons, deuterons, etc.) – 21.65.+f Nuclear matter – 24.10.Cn Many-body theory

1 Introduction

The equation of state (EOS) of neutron-rich matter is a source of important theoretical predictions on the properties of neutron stars, heavy-ion collisions (HIC) and nuclei at the neutron drip line [1]. The general interest has been focussed mainly on the symmetry energy, including its dependence on the baryonic density. Studies of neutron star cooling [2], spin-polarized states [3], collective flows and isospin distillation in HIC [4–6] have stressed that those phenomena are very sensitive to the values of the symmetry energy in the respective density domains. The EOS of isospin-asymmetric nuclear matter (ANM) has been recently studied in the framework of the Brueckner-Bethe-Goldstone (BBG) theory [7,8]. The convergence of the BBG hole line expansion has been assessed in recent times with high accuracy [9], even if the saturation properties of nuclear matter are not reproduced. It is commonly recognized that the missing saturation is due to the modelling of nucleons as structureless particles interacting via a bare two-body force (2BF). One thus has to introduce three-body forces (3BF). The first microscopic model of 3BF was the Fujita-Miyazawa model [10] where the isobar $\Delta(1232)$ is excited in a pion exchange interaction between two nucleons. The model was later extended to the $N(1440)$ Roper resonance [11]. It has been also recognized that the main relativistic effect introduced by the Dirac-Brueckner approach is the excitation of the negative-energy states of the Fermi sea which can be described in terms of a 3BF [12] as well.

The above-mentioned 3BF components have a strong saturating effect as already shown by a Brueckner-Hartree-Fock (BHF) calculation using the Paris potential as 2BF [11]. This 3BF has been re-adopted in ref. [13] in combination with the Argonne V_{18} [14] as two-body component. In ref. [15] the EOS of pure neutron matter was discussed and a preliminary prediction was given for the symmetry energy based on the shift between the energy of pure neutron matter and symmetric nuclear matter. However, one may argue that 3BF could modify the β^2 law fulfilled by the binding energy of ANM, especially at high density, and higher-order terms in the β expansion could significantly limit the role played by the symmetry

[a] e-mail: lombardo@lns.infn.it

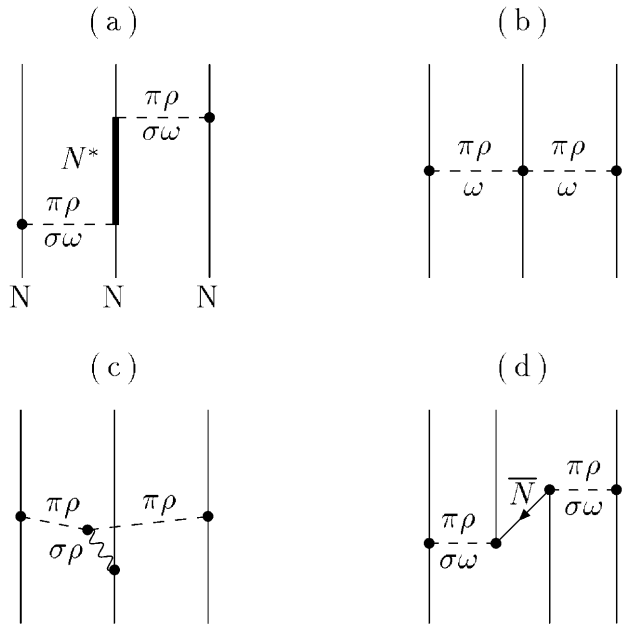

Fig. 1. Diagrams of the microscopic 3BF adopted in the present calculation (see ref. [11]). Diagram (c) was not included.

energy in describing the isospin effects. These considerations require to extend the calculation of the EOS to the full asymmetry range $0 < \beta < 1$ and up to high enough baryonic density. In this paper we will present the results of such a calculation. After describing the model of 3BF (sect. 2) we shall focus on the 3BF effects on binding energy, symmetry energy and single-particle properties of ANM (sect. 3). Then a few direct applications in the neutron star cooling and in the isospin properties of HIC will be shortly discussed along with a comparison with other approaches (sect. 4).

2 Isospin-dependent 3BF

The microscopic 3BF adopted in the present calculation is based on the meson exchange current approach. It is described in full detail in ref. [11]. The new meson parameters calculated to meet the self-consistent requirement with the adopted AV_{18} 2BF are reported in ref. [13].

It has been shown [11,13] that the main contributions to 3BF arise from the two-meson exchange part of the nucleon-nucleon (NN) interaction medium modified by the intermediate virtual excitation of nucleon resonances (isobar $\Delta(1232)$ and Roper $N(1440)$) (fig. 1a) and from the two-meson exchange part with nucleon-antinucleon virtual excitations (fig. 1d). The latter contains the relativistic effects associated with the dressed spinors of the Dirac-Brueckner approach [16]. The terms associated with the non-linear π-nucleon coupling required by the chiral symmetry [17] play a minor role, especially above the saturation density, where heavy mesons (σ and ω) are dominating over the 2π-3BF (fig. 1b, diagrams without heavy mesons). The contribution due to meson-meson coupling (fig. 1c) is negligible [11] and was therefore not considered in the present calculations. In the context of non-relativistic approaches phenomenological 3BF have also been introduced [18] in the calculations of nuclear matter. They are modelled according to the saturation properties of nuclear matter and/or the binding energies of light nuclei. Good agreement between microscopic and phenomenological 3BF is found only when the latter is treated within the Brueckner approach [19].

The general Brueckner formalism for ANM with 2BFs is described in ref. [8]. The rigorous procedure to include 3BF would require to solve the Bethe-Faddeev equation with a 3BF much the same as already done to calculate the three-body clusters in the BBG hole line expansion [9]. Since at the present time this appears a formidable task, we follow a simplified procedure based on converting the 3BF into an effective two-body force via a suitable integration over the degrees of freedom of the third nucleon. The integral is weighted over the correlation function of the third nucleon with respect to the two others [11,13]. The effective 2BF for ANM is defined as

$$\begin{aligned}\langle \vec{r}_1\vec{r}_2|\ V_3^{\tau_1\tau_2}\ |\vec{r}_1{}'\vec{r}_2{}'\rangle = \frac{1}{4}\sum_{\tau_3}\sum_{\sigma_3}\sum_{\rm n}\int {\rm d}\vec{r}_3{\rm d}\vec{r}_3{}'\phi^*_{\rm n}(\tau_3\vec{r}_3{}')\\ \times(1-\eta_{\tau_1,\tau_3}(r'_{13}))(1-\eta_{\tau_2,\tau_3}(r'_{23}))\\ \times W_3(\vec{r}_1{}'\vec{r}_2{}'\vec{r}_3{}'|\vec{r}_1\vec{r}_2\vec{r}_3)\phi_{\rm n}(\tau_3 r_3)\\ \times(1-\eta_{\tau_1,\tau_3}(r_{13}))(1-\eta_{\tau_2,\tau_3}(r_{23}))\,. \qquad (1)\end{aligned}$$

The function $\eta_{\tau_1\tau_2}(r)$ is the average over spin and momenta in the Fermi sea of the defect function of which only the most important partial-wave components have been included, *i.e.*, the $^1S_0$ and $^3S_1$ partial waves.

The transformation of the 3BF to an effective 2BF entails a self-consistent coupling between the 3BF and the Brueckner procedure of solving the Brueckner-Bethe-Goldstone equations. One first calculates the correlation function with only the 2BF and then builds up the effective 3BF which in turn is added to the 2BF, and again the correlation function. This procedure is repeated up to the convergence is reached. As previously mentioned the bare 2BF adopted in the calculations is the charge-dependent force AV_{18}. The partial-wave expansion of the full interaction has been truncated at $l_{\max} = 6$.

3 Numerical results

The EOS of ANM has been calculated spanning the whole asymmetry range with a step-size $\Delta\beta = 0.2$ in a density domain up to 0.45 fm^{-3}. The case of symmetric nuclear matter ($\beta = 0$) is discussed in ref. [15] (the saturation properties are reported in table 1). The results for ANM are displayed in fig. 2 for both cases with (left panel) and without (right panel) 3BF. In this figure the energy shift for asymmetric-to-symmetric nuclear matter is plotted *vs.* β^2. The individual runs (symbols in the figure) are depicted along with their linear fits (solid lines) performed

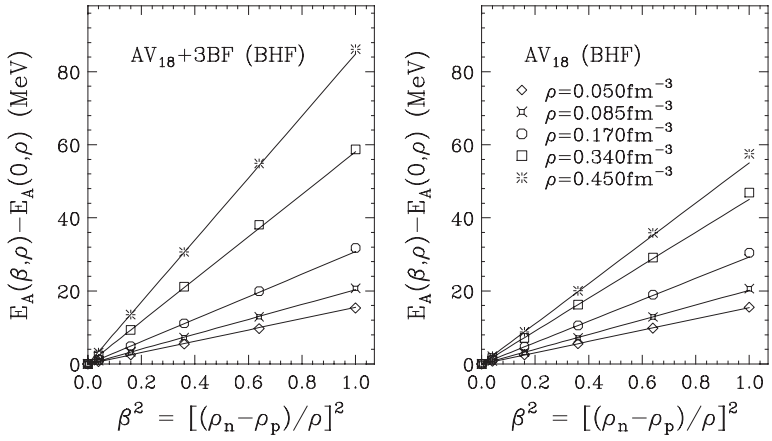

Fig. 2. Energy per nucleon of asymmetric nuclear matter in the range $0 \leq \beta^2 \leq 1$ at four densities as compared to the parabolic fits (straight lines) obtained from the first three values of β (0.0, 0.2, 0.4). Left panel: BHF predictions using AV_{18} plus the 3BF. Right panel: BHF results with only pure AV_{18} 2BF.

Table 1. Equilibrium density of asymmetric nuclear matter, incompressibility and energy per nucleon at equilibrium density corresponding to four different values of the asymmetry β. Density units are fm^{-3}, K and E_A units are MeV.

	$AV_{18}+3$BF			AV_{18}		
β	$\rho_{\rm eq}$	$K(\rho_{\rm eq})$	$E_A(\rho_{\rm eq})$	$\rho_{\rm eq}$	$K(\rho_{\rm eq})$	$E_A(\rho_{\rm eq})$
0.0	0.198	207.84	−15.05	0.265	232.35	−18.25
0.2	0.193	195.34	−13.82	0.259	228.54	−16.74
0.4	0.165	142.33	−9.93	0.226	177.49	−12.38
0.6	0.120	85.28	−4.44	0.172	96.1	−5.89

with only the first three values of the asymmetry parameter β. From the comparison between the two sets of calculations one may notice that, despite its strongly density-dependent repulsive effect, the 3BF does not violate the β^2 law fulfilled already with only 2BF. The rather good agreement between the symbols and the corresponding lines (the maximum deviation is 6%) indicates the high quality of the β^2 law up to the largest densities. This is a quite astonishing result because the 3BF introduces a strong density and isospin dependence, making the in-medium NN interaction quite different from the bare 2BF. On the other hand, this is indeed a quite desirable result for two reasons. First, this is in agreement with previous studies [7, 8,20,21] using a charge-independent 2BF and provides a strong support for using the empirical β^2 law to describe isospin effects. Second, it imposes also strict theoretical constraints on the phenomenological nuclear forces when extended to ANM. We have in mind the Skyrme forces which have been fit at the saturation point of symmetric nuclear matter and include an effective density-dependent term to simulate the effects of 3BF.

In table 1 the saturation properties of ANM are shown with and without 3BF. One may just notice that 3BF reduces the compression modulus at equilibrium density despite the strong enhancement of the curvature of the corresponding EOS. This is due to the fact that it is also proportional to the square of the saturation density, which turns out to be very much reduced.

The symmetry energy is defined as

$$E_{\rm sym}(\rho) \quad = \quad \frac{1}{2}\left[\frac{\partial^2 E_A(\beta,\rho)}{\partial\beta^2}\right]_{\beta=0}. \qquad (2)$$

Due to the simple β^2 law the symmetry energy can be equivalently calculated as the difference between the energy per nucleon of pure neutron matter and symmetric nuclear matter, *i.e.*,

$$E_{\rm sym}(\rho) \; = \; E_A(\rho,1) - E_A(\rho,0)\,. \qquad (3)$$

Figure 3 shows the effect of the 3BF on the symmetry energy in the density domain considered in this study. At the saturation density the two values do not significantly differ from one another: 30.71 MeV (3BF included) and 29.28 MeV (no 3BF). Both are in good agreement with the empirical value 30. ± 4 MeV extracted from the nuclear mass table [22]. Above $\rho_{\rm eq}$ the 3BF brings about a strong enhancement of the symmetry energy since it is strongly repulsive at high density. Both curves, with and without the 3BF, have been parametrized by simple power laws as follows:

– BHF with pure AV_{18} 2BF:

$$E_{\rm sym} = 30.7u^{0.58}\,; \qquad (4)$$

– BHF using AV_{18} plus the 3BF:

$$\begin{aligned} E_{\rm sym} &= 30.71u^{0.6}\,, && u \leq 1 \\ &= 30.71 + 18.42(u-1) + 9(u-1)^2\,, && u > 1\,, \end{aligned} \qquad (5)$$

where $u = \rho/\rho_0$, and $\rho_0 = 0.17$ fm^{-3} is the empirical saturation density. The above simple relations, plotted in fig. 3 (right panel), may be useful in HIC simulations.

In fig. 3 (left panel) $E_{\rm sym}$ *vs.* density is compared with other approaches. Despite the overall agreement with

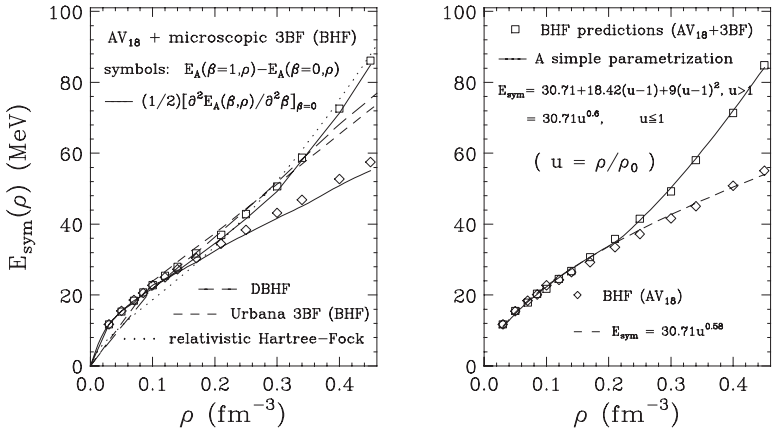

Fig. 3. Symmetry energy *vs.* density. The left panel shows a comparison among different approaches: the BHF predictions with 3BF (upper solid curve) and without 3BF (lower solid curve) are obtained from the slopes of fig. 2 (while symbols are the values approximated by eq. (3)); the long-dashed curve corresponds to the result of the DBHF approach from ref. [20]. The short-dashed curve is that of BHF calculation using the phenomenological Urbana 3BF in ref. [19], where $E_{\rm sym}$ is obtained from eq. (3). The dotted curve is the prediction of the relativistic Hartree-Fock approach taken from ref. [23]. The right panel shows simple parametrizations of the present results with (solid line) and without (dashed line) 3BF.

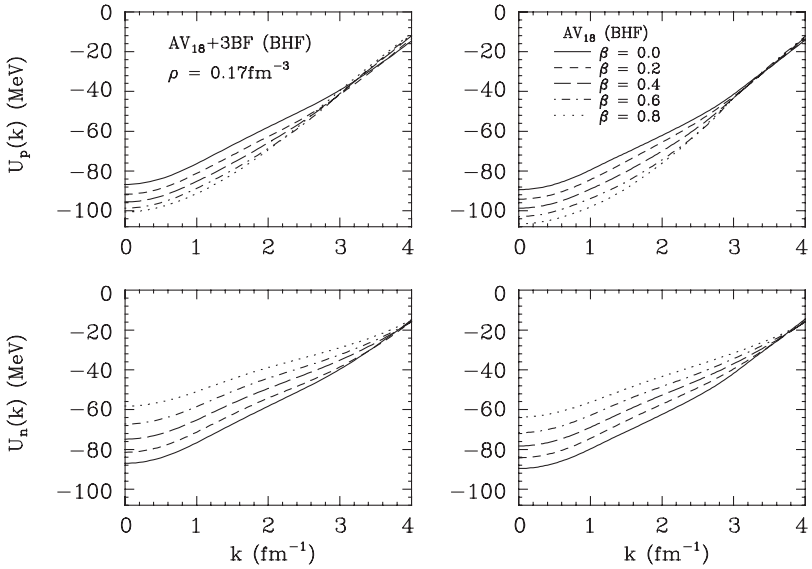

Fig. 4. Proton and neutron mean fields in asymmetric nuclear matter at $\rho = 0.17$ fm^{-3} for five different asymmetries. The left part shows the proton mean-field (upper panel) and the neutron one (lower panel), respectively, *vs.* momentum using AV_{18} plus the 3BF. The right part shows the corresponding results without the 3BF.

the predictions of the relativistic mean-field (RMF) theory [23] and the Dirac-Brueckner-Hartree-Fock approach (DBHF) [20], the density dependence is found to be rather different. Both RMF and DBHF theories predict an almost linear variation of $E_{\rm sym}$ *vs.* density. Instead, in the present BHF calculation with the 3BF, $E_{\rm sym}$ slowly increases at relatively low density, say from $\rho \simeq 0.03$ fm^{-3} to $\rho \simeq 0.25$ fm^{-3}. Such a slow variation is also found in a density region up to $\rho \simeq 0.2$ fm^{-3} in ref. [24] from the three-loop approximation of chiral perturbation theory. In this density region, the shape of $E_{\rm sym}$ plays an important role in the study of the isospin effects in HIC at intermediate energy as discussed later. On the contrary, in the relatively high-density domain, *i.e.*, $\rho \geq 0.3$ fm^{-3}, the present calculation predicts a steeper density dependence than DBHF and RMF.

Due to the isospin effect, the proton and neutron single-particle potentials are different. As discussed in ref. [8], where only the charge-independent AV_{14} 2BF was used, the attractive $T = 0$ SD channel contribution in the two-body NN interaction mainly drives the isospin dependence of the proton and neutron mean fields. As a result, the proton mean field becomes more attractive and the neutron one more repulsive with increasing asymmetry. In the BHF approximation both proton and neutron mean fields vary linearly with the asymmetry parameter β, which is in keeping with the β^2-dependence of the energy per nucleon. A linear potential was introduced

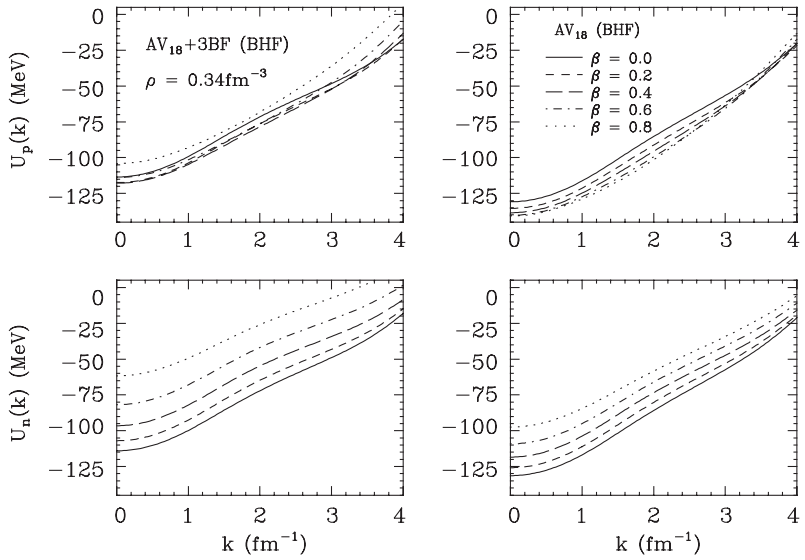

Fig. 5. The same as in fig. 4 for $\rho = 0.34$ fm^{-3}.

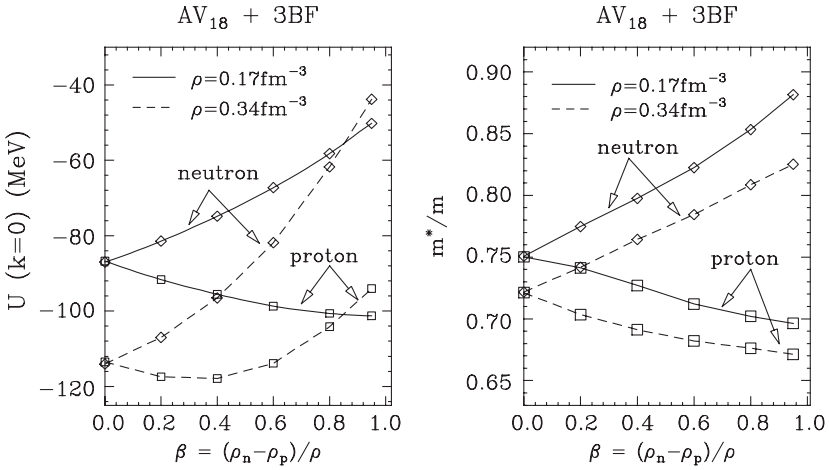

Fig. 6. Left panel: Isospin variation of proton and neutron mean fields at a fixed momentum $k = 0$ for two densities $\rho = 0.17$ and 0.34 fm^{-3}. Right panel: isospin dependence of proton and neutron effective masses calculated at their respective Fermi momenta. The results in both panels are calculated using AV_{18} plus the 3BF.

phenomenologically long ago [25] and is referred to as the Lane potential. Due to the importance of the single-particle properties such as mean field and effective mass in HIC physics [26,27], it is of some interest to explore the effect of the 3BF on such quantities. The proton and neutron mean fields are shown as a function of momentum k at different asymmetries $\beta = 0$, 0.2, 0.4, 0.6, 0.8 in fig. 4 for the saturation density $\rho = 0.17$ fm^{-3} and in fig. 5 for high density $\rho = 0.34$ fm^{-3}. In both figures the left panels display the results using AV_{18} plus 3BF while the right panels give the results using pure AV_{18}. As expected, the 3BF adds a repulsive contribution to both proton and neutron mean fields at all asymmetries. At relatively low density (fig. 4), the proton mean field with 3BF becomes more attractive, which is in agreement with the 2BF prediction. However, the validity of the linear Lane assumption is broken by 3BF as more clearly seen in the left panel of fig. 6, where the isospin variation of the proton and neutron mean fields are plotted at momentum $k = 0$. At relatively high density (figs. 5 and 6), the 3BF effect becomes much more pronounced and in fact it brings about a strong deviation from the linear Lane assumption. The neutron mean field rises up more rapidly as compared to the results with pure AV_{18}. The same happens to the proton potential which at a certain asymmetry becomes even more repulsive. This remarkable result can be explained by the competition between the isospin dependence of the 3BF and the contribution from the attractive $T = 0$ SD channel. As increasing isospin asymmetry the 3BF repulsion starts to compete with the $T = 0$ SD channel 2BF attraction, and becomes the dominant one at high enough density.

The effective mass for neutron or proton is defined as [28]

$$\frac{m^*_\tau(k)}{m} = \frac{k}{m}\left(\frac{\mathrm{d}\epsilon^\tau(k)}{\mathrm{d}k}\right)^{-1}, \qquad (6)$$

where $\epsilon^\tau(k) = \hbar^2k^2/2m + U_\tau(k)$ is the neutron (τ = n) or proton (τ = p) single-particle energy. The momentum dependence of m^* is featured by a wide bump inside the Fermi sphere due to the high-probability amplitude for particle-hole excitations near the Fermi surface. In fact such a bump originates from the energy dependence of the mass operator and is related to the E-mass as discussed in ref. [28]. The isospin dependence of the proton and neutron effective masses at their respective Fermi momenta $k_{\rm F}^{\rm p}$ and $k_{\rm F}^{\rm n}$ are given in the right panel of fig. 6. The 3BF does not affect the linear scissor-shaped behavior observed in the previous calculations using a pure 2BF [7,8]. One should notice that the isospin effect on neutron and proton effective masses in the Brueckner approach goes the other way around than in the RMF approach [23]. This discrepancy is to be understood taking also into account the different definitions of effective mass in the two approaches.

4 Summary and discussion

In the present work the microscopic 3BF based on the meson exchange current approach has been extended and applied to isospin ANM in the framework of the Brueckner theory. The 3BF effects on the isospin dependence of both the nuclear EOS and single-particle properties have been investigated.

The obtained results confirm the validity of the β^2 law for the energy per nucleon in the entire range of isospin asymmetry and up to high density, in spite of the strong isospin and density dependence of the 3BF. As a consequence, the isospin effects in ANM are just driven by the symmetry energy as in the case with only the 2BF. The vanishing of higher powers in the β^2 expansion also supports the simple recipe frequently adopted to extract the symmetry energy from the two limiting cases of symmetric nuclear matter and pure neutron matter. It also constrains theoretically the phenomenological interactions, such as the Skyrme forces which take into account the effect of 3BF by a density-dependent term.

As expected, the 3BF improves the saturation properties of symmetric nuclear matter by shifting the equilibrium density close to the empirical value. At relatively low density, the 3BF effect on the nuclear symmetry energy is quite small. On the contrary, at high density, it brings about a strong enhancement and consequently the symmetry energy rises with density more steeply than the corresponding 2BF prediction. The non-linear increase of symmetry energy at high density has also been observed in a recent relativistic Hartree-Fock calculation [23] as the "Fock" exchange effect of the non-linear scalar self-interactions. But in the same ref. [23] it is also shown that at sub-nuclear densities the Fock contribution could result in a softening of the symmetry potential term.

The density dependence of the symmetry energy has been parametrized for the sake of the application to HIC with very neutron-rich ions. It has already been shown that isospin fractionation [4,29] in multifragmentation events is very sensitive to the density dependence of $E_{\rm sym}$ in the low-density region. In particular, in ref. [30] it is shown that using an isospin stiff nuclear EOS with a symmetry energy curvature equal to -69 MeV (very close to the present value of -66 MeV) leads to a value for the liquid-to-gas isospin asymmetry ratio which is consistent with the experimental prediction [5]. An isospin scaling has been proposed in multifragmentation events of HIC, which turns out to be also very sensitive to the density dependence of $E_{\rm sym}$. Using the expanding evaporating source model and adopting for $E_{\rm sym}$ the simple parametrization $C{\cdot}(\rho/\rho_0)^\gamma$ the fragment data can be fairly well reproduced using $\gamma = 0.6$ [31], which coincides with the fit of our microscopic value (cf. eq. (5)).

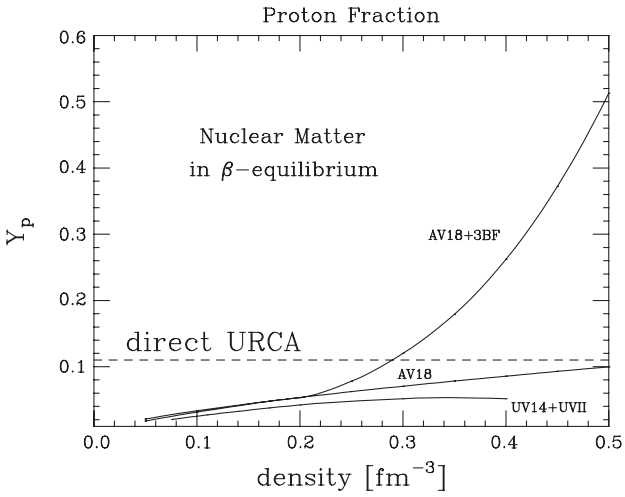

Fig. 7. Proton fraction in β-equilibrium nuclear matter calculated in the BHF approximation with 2BF (AV_{18}) and 2BF plus 3BF ($AV_{18}+3$BF) in comparison with a variational calculation using Urbana 2BF and 3BF ($UV_{14}+UVII$). The dashed horizontal line is the threshold for direct URCA processes estimated in ref. [34].

The preequilibrium particle emission [32,33] and collective flows [4,6] can instead probe the symmetry energy in the range of high density, say up to two times the saturation density. The calculation of the particle production rates supports an isospin stiff EOS in agreement with our prediction.

In the high-density range the symmetry energy is also relevant to the study of the neutron star properties such as the cooling mechanism. In fact, a steep increase of $E_{\rm sym}$ with density favours the direct URCA processes [2]. In fig. 7 the proton fraction is reported for β-equilibrium nuclear matter in different approximations. The threshold of direct URCA processes is only reached by the results with 3BF and this happens at a reasonably low value of the neutron star density.

As to the single-particle properties, the effect of the 3BF is to add an extra repulsion to both proton and neutron mean fields so that the linear Lane assumption breaks down slightly around the saturation density but quite strongly at high density. However, the scissor-shaped behavior of the proton and neutron effective masses *vs.* β remains unchanged being the momentum dependence of

the mean fields rather insensitive to 3BF. In a calculation not reported here it was found that the 3BF affects only slightly the *rearrangement* contribution to the nuclear mean field and cannot improve the fulfillment of Hughenoltz-Van Hove theorem (see ref. [8]). This requires to go beyond the BHF approximation in the expansion of mass operator that is a work still in progress.

One of us (WZ) would like to thank INFN-LNS and the Physics Department of the Catania University (Italy) for their hospitality during the preparation of the present work. This work has been supported in part by the Chinese Academy of Science, within the *One Hundred Person Project*, the Major State Basic Research Development Program of China under No. G2000077400.

References

1. For a recent review see: M. Baldo (Editor), *Nuclear Methods and the Nuclear Equation of State* (World Scientific, 1999).
2. J.M. Lattimer, C.J. Pethick, M. Prakash, P. Haensel, Phys. Rev. Lett. **66**, 2701 (1991).
3. J. Margueron, PhD Thesis, IPNO-T-01-07 (2001).
4. B.A. Li, Phys. Rev. Lett. **85**, 4221 (2000).
5. H.S. Xu *et al.*, Phys. Rev. Lett. **85**, 1908 (2000).
6. L. Scalone, M. Colonna, M. Di Toro, Phys. Lett. B **461**, 9 (1999).
7. I. Bombaci, U. Lombardo, Phys. Rev. C **44**, 1892 (1991).
8. W. Zuo, I. Bombaci, U. Lombardo, Phys. Rev. C **60**, 024605 (1999).
9. H.Q. Song, M. Baldo, G. Giansiracusa, U. Lombardo, Phys. Rev. Lett. **81**, 1584 (1998); M. Baldo, G. Giansiracusa, U. Lombardo, H.Q. Song, Phys. Lett. B **473**, 1 (2000).
10. J. Fujita, H. Miyazawa, Prog. Theor. Phys. **17**, 360; 366 (1957).
11. P. Grange, A. Lejeune, M. Martzolff, J.-F. Mathiot, Phys. Rev. C **40**, 1040 (1989).
12. G.E. Brown, W. Weise, G. Baym, J. Speth, Comments Nucl. Phys. **17**, 39 (1987).
13. W. Zuo, A. Lejeune, U. Lombardo, J. -F. Mathiot, Nucl. Phys. A **706**, 418 (2002).
14. R.B. Wiringa, V.G.J. Stoks, R. Schiavilla, Phys. Rev. C **51**, 38 (1995).
15. A. Lejeune, U. Lombardo, W. Zuo, Phys. Lett. **477**, 45 (2000).
16. R. Brockmann, R. Machleidt, *The Dirac-Brueckner Approach* in *Nuclear Methods and Nuclear Equation of State*, edited by M. Baldo (World Scientific, 1999) p. 121.
17. E. Epelbaum, Ulf-G. Meissner, W. Glöckle, C. Elster, H. Kamada, A. Nogga, H. Witala, *Proceedings of the Conference on Mesons and Light Nuclei, Prag, July 2001*, and references therein, nucl-th/0109065.
18. For a recent review see: S.C. Pieper, V.R. Pandharipande, R.B. Wiringa, J. Carson, Phys. Rev. C **64**, 014001 (2001).
19. M. Baldo, I. Bombaci, G.F. Burgio, Astron. Astrophys. **328**, 274 (1997).
20. C.H. Lee, T.T.S. Kuo, G.Q. Li, G.E. Brown, Phys. Rev. C **57**, 3488 (1998).
21. H. Huber, F. Weber, M.K. Wiegel, Phys. Rev. C **51**, 1790 (1995); **57**, 3484 (1998).
22. P.E. Haustein, At. Data Nucl. Data Tables **39**, 185 (1988).
23. B. Liu, V. Greco, F. Matera, M. Colonna, M. Di Toro, Phys. Rev. C **65**, 045201 (2002).
24. N. Kaiser, S. Fritsch, W. Weise, *Chiral Dynamics and Nuclear Matter*, arXiv:nucl-th/0105057.
25. A.M. Lane, Nucl. Phys. **35**, 676 (1962).
26. G.F. Bertsch, S. Das Gupta, Phys. Rep. **160**, 189 (1988).
27. W. Cassing, V. Metag, U. Mosel, K. Nitta, Phys. Rep. **188**, 363 (1990).
28. J.P. Jeukenne, A. Lejeune, C. Mahaux, Phys. Rep. C **25**, 83 (1976); P. Grange, J. Cugnon, A. Lejeune, Nucl. Phys. A **473**, 365 (1987).
29. M. Colonna, M. Di Toro, A.B. Larionov, Phys. Lett. B **428**, 1 (1998).
30. B.A. Li, C.M. Ko, Nucl. Phys. A **618**, 498 (1997).
31. M.B. Tsang, W.A. Friedman, C.K. Gelbke, W.G. Lynch, G. Verde, H. Xu, Phys. Rev. Lett. **86**, 5023 (2001).
32. B.A. Li, C.M. Ko, W. Bauer, Int. J. Mod. Phys. E **7**, 147 (1998).
33. B.A. Li, C.M. Ko, Z.Z. Ren, Phys. Rev. Lett. **78**, 1644 (1997).
34. R.B. Wiringa, V. Fiks, A. Fabrocini, Phys. Rev. C **38**, 1010 (1988).